Effect of Material Frame Rotation on the Hardening of an Anisotropic Material in Simple Shear Tests

Kelin Chen
Research Center for Mechanics of Solids,
Structures and Materials,
The University of Texas at Austin,
WRW 110,
Austin, TX 78712

Stelios Kyriakides[1]
Research Center for Mechanics of Solids,
Structures and Materials,
The University of Texas at Austin,
WRW 110,
Austin, TX 78712
e-mail: skk@mail.utexas.edu

Martin Scales
Research Center for Mechanics of Solids,
Structures and Materials,
The University of Texas at Austin,
WRW 110,
Austin, TX 78712

The shear stress–strain response of an aluminum alloy is measured to a shear strain of the order of one using a pure torsion experiment on a thin-walled tube. The material exhibits plastic anisotropy that is established through a separate set of biaxial experiments on the same tube stock. The results are used to calibrate Hill's quadratic anisotropic yield function. It is shown that because in simple shear the material axes rotate during deformation, this anisotropy progressively reduces the material tangent modulus. A parametric study demonstrates that the stress–strain response extracted from a simple shear test can be influenced significantly by the anisotropy parameters. It is thus concluded that the material axes rotation inherent to simple shear tests must be included in the analysis of such experiments when the material exhibits anisotropy. [DOI: 10.1115/1.4041320]

Keywords: simple shear, anisotropy, material hardening, torsion

1 Introduction

The analysis of processes involving large deformations, such as sheet metal forming, crushing of thin-walled tubular structures for energy absorption purposes, and modeling of ductile failure require material stress–strain responses to large strains. The material response is commonly measured in a uniaxial tension test, which usually necks at a strain of a few percent. The postnecking response can be extracted iteratively by using a numerical simulation of the test in conjunction with an appropriate constitutive model to simulate the necking (e.g., see Ref. [1]). For sheet metal, the hydraulic bulge test provides a direct way of establishing the material response to much larger strains than the uniaxial tension test but is also limited by instability (e.g., see Ref. [2] and references therein). Simple shear tests, on the other hand, remain free of instabilities to large strains and therefore offer an attractive alternative (e.g., see Refs. [3–5]; and review in Ref. [6]). It is now well established that for all three methods the extracted material response is influenced by the constitutive model adopted (i.e., quadratic versus nonquadratic isotropic and anisotropic yield functions [1,2,7–9]). A less well-known additional complication affecting the simple shear tests is that the material axes can rotate during shearing, which has consequences if the material exhibits plastic anisotropy (Ch. XII-1 in Ref. [10]). In this brief note, this effect is demonstrated through the extraction of the material hardening for an anisotropic Al-alloy from a pure torsion test on a thin-walled circular tube.

2 Experimental

A pure torsion experiment was performed on a seamless 2.0×0.187 in (51×4.75 mm) Al-6061-T6 tube. The specimen is machined on the OD in a way that minimizes wall eccentricity; it has a 0.400 in (10.2 mm) test section with a wall thickness of 0.0461 in (1.17 mm) machined at midspan as shown in Fig. 1 (thickness chosen to delay buckling). The experiment was performed in an axial-torsional servohydraulic testing machine using the setup shown in Fig. 2 in Scales et al. [11]. The specimen was twisted under rotation control producing a shear strain rate of approximately 2×10^{-4} s^{-1}, while the axial load was prescribed to remain at zero.

The shear stress, τ, is calculated directly from the recorded torque using the thin-walled geometry of the test section. The deformation in the test section was monitored using stereo digital image correlation with the appropriate resolution (see Ref. [11]). The ARAMIS software provides the deformation gradient, $\boldsymbol{F}$. The deformation in the test section was found to remain quite uniform but $\boldsymbol{F}$ was averaged over a zone 0.2×0.4 in (5.1×10.2 mm) in the center of the test section. For the case of simple shear, $\boldsymbol{F}$ is given by

$$\boldsymbol{F} = \begin{bmatrix} 1 & \gamma & 0 \\ 0 & 1 & 0 \\ 0 & 0 & 1 \end{bmatrix} \tag{1}$$

where γ is defined in Fig. 2.

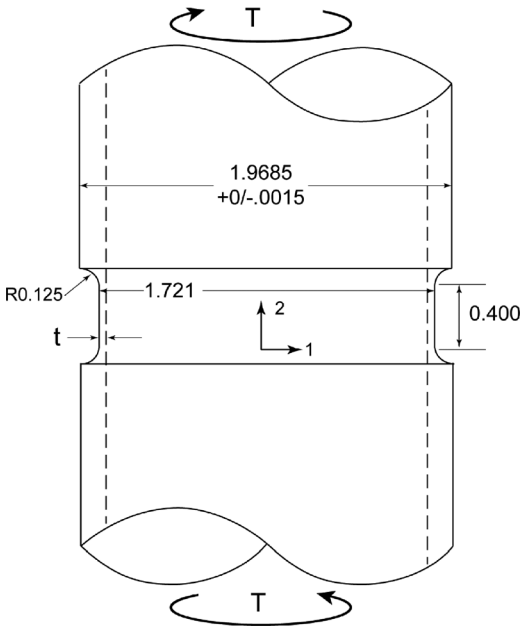

Fig. 1 Tubular test specimen loaded in pure torsion generating simple shear in the thin-walled test section (dimensions in inches; 1 in = 25.4 mm)

[1]Corresponding author.

Contributed by the Applied Mechanics Division of ASME for publication in the JOURNAL OF APPLIED MECHANICS. Manuscript received July 9, 2018; final manuscript received August 21, 2018; published online September 21, 2018. Assoc. Editor: Shaoxing Qu.

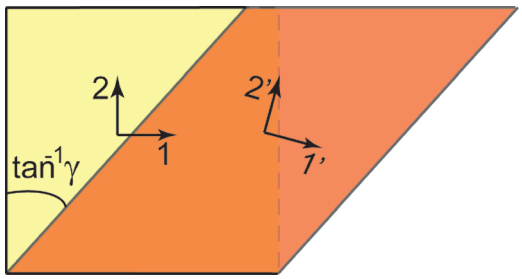

Fig. 2 Material element under simple shear; shown are the initial and rotated material axes

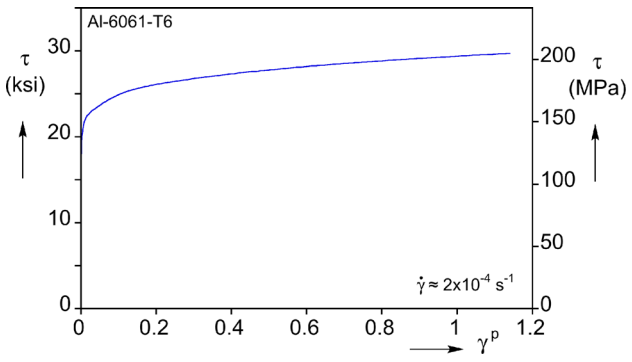

Fig. 3 Measured shear stress–plastic shear strain ($\tau-\gamma^p$) response for the Al-6061-T6 tube analyzed

The instantaneous strain tensor is then given by

$$d\boldsymbol{\varepsilon} = \mathrm{sym}(d\boldsymbol{F}\boldsymbol{F}^{-1}) = \begin{bmatrix} 0 & d\gamma/2 & 0 \\ d\gamma/2 & 0 & 0 \\ 0 & 0 & 0 \end{bmatrix} \tag{2}$$

Figure 3 shows the shear stress–plastic shear strain ($\tau - \gamma^p$) response measured in this experiment. It extends to a strain of just under 1.2 and exhibits hardening throughout.

3 Material Response

The pure torsion test was part of a larger study aimed at establishing the response and failure of this tubular product under a set of radial paths of combined shear and tension (akin to those in Ref. [11]). The material was found to yield anisotropically. Eight shear-tension tests of varying stress ratios and seven pressure-tension tests were used to quantify the material anisotropy using the nonquadratic Yld04-three-dimensional model [7] with an exponent of 8, which is preferred for Al-alloys. However, for the narrow purposes of this study, the same data were used to also calibrate the quadratic Hill-1948 (H-48) [12] anisotropic yield function, in order to facilitate a simple study of the sensitivity to the anisotropy parameters. For the present stress state, H-48 can be written as

$$\sigma_e = \left[\sigma_{11}^2 - \left(1 + \frac{1}{S_2^2} - \frac{1}{S_3^2}\right)\sigma_{11}\sigma_{22} + \frac{1}{S_2^2}\sigma_{22}^2 + \frac{3}{S_{12}^2}\sigma_{12}^2\right]^{1/2} \tag{3a}$$

where S_{ij} are the ratios of the following yield stresses:

$$S_2 = \sigma_{2o}/\sigma_{1o},\ \ S_3 = \sigma_{3o}/\sigma_{1o},\ \ S_{12} = \sqrt{3}\sigma_{12o}/\sigma_{1o} \tag{3b}$$

S_{ij} were determined by minimizing the sum of set of weighted error functions as in Refs. [1,2], and [7] at plastic work of 1000 psi (6.897 MPa) for all experiments. The process produced the following values for the anisotropy parameters:

$$S_2 = 1.01,\ \ S_3 = 0.97,\ \ S_{12} = 0.93$$

This calibration will be used to demonstrate the effect of anisotropy on the extracted material response.

The incremental spin tensor is given by

$$d\boldsymbol{\omega} = \mathrm{skewsym}(d\boldsymbol{F}\boldsymbol{F}^{-1}) = \begin{bmatrix} 0 & d\gamma/2 & 0 \\ -d\gamma/2 & 0 & 0 \\ 0 & 0 & 0 \end{bmatrix} \tag{4a}$$

which integrates to

$$\boldsymbol{\omega} = \begin{bmatrix} 0 & \gamma/2 & 0 \\ -\gamma/2 & 0 & 0 \\ 0 & 0 & 0 \end{bmatrix} \tag{4b}$$

Thus, the transformation tensor for the material frame (MF) becomes

$$\boldsymbol{A} = \begin{bmatrix} \cos\gamma/2 & -\sin\gamma/2 & 0 \\ \sin\gamma/2 & \cos\gamma/2 & 0 \\ 0 & 0 & 1 \end{bmatrix} \tag{5}$$

The stress, when rotated into the material frame, is then

$$\boldsymbol{\sigma}' = \boldsymbol{A}\sigma\boldsymbol{A}^T = \tau\begin{bmatrix} -\sin\gamma & \cos\gamma & 0 \\ \cos\gamma & \sin\gamma & 0 \\ 0 & 0 & 1 \end{bmatrix} \tag{6}$$

For the anisotropic material in Eq. (3), the equivalent stress in the material frame then becomes

$$\sigma_e = \sigma_e(\sigma'_{ij}, S_2, S_3, S_{12}) \tag{7a}$$

or

$$\sigma_e = \tau\left[\frac{3}{S_{12}^2} + \left(2 + \frac{2}{S_2^2} - \frac{1}{S_3^2} - \frac{3}{S_{12}^2}\right)\sin^2\gamma\right]^{1/2} \tag{7b}$$

This is used to evaluate the work compatible plastic equivalent strain increment from

$$d\varepsilon_e^p = \frac{\tau d\gamma^p}{\sigma_e} \tag{8a}$$

which in the material frame becomes

$$d\varepsilon_e^p = \frac{d\gamma^p}{\left[\frac{3}{S_{12}^2} + \left(2 + \frac{2}{S_2^2} - \frac{1}{S_3^2} - \frac{3}{S_{12}^2}\right)\sin^2\gamma^p\right]^{1/2}} \tag{8b}$$

(the elastic component of γ is neglected). This integrates as an elliptic integral of the first kind. In the reference frame (RF), on the other hand

$$d\varepsilon_e^p = \frac{S_{12}}{\sqrt{3}}d\gamma^p \tag{8c}$$

which integrates directly.

If the material yields isotropically, Eq. (3) reduces to von Mises (vM), is invariant to transformation and

$$\sigma_e|_{\mathrm{vM}} = \sqrt{3}\,\tau \tag{9a}$$

$$d\varepsilon_e^p\Big|_{\mathrm{vM}} = \frac{d\gamma^p}{\sqrt{3}} \tag{9b}$$

which also integrates directly.

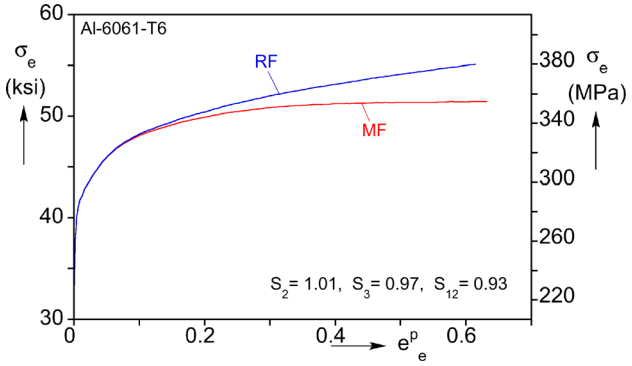

Fig. 4 The material and reference frame equivalent stress–equivalent plastic strain responses extracted from the measured $\tau-\gamma^p$ response. Included are the calibrated Hill-48 anisotropy constants.

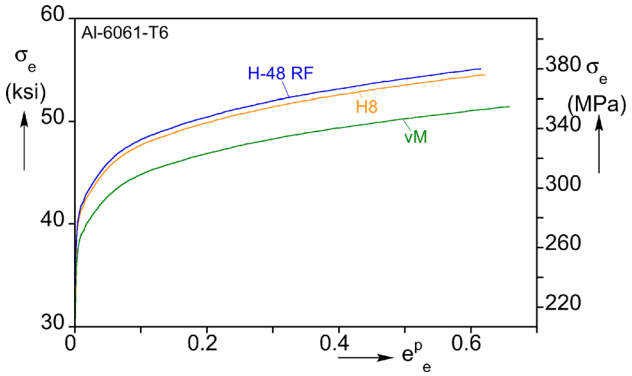

Fig. 5 Comparison of the Reference Frame equivalent stress–equivalent plastic strain response with the von Mises and Hosford responses when the anisotropy is neglected

To facilitate a comparison with the quadratic yield functions, we include the equivalent stress for the isotropic Hosford yield function [13] with exponent 8 (H8) which is given by

$$\sigma_e|_{\mathrm{H8}} = (2^7+1)^{1/8}\,\tau \tag{10a}$$

$$d\varepsilon_e^p\Big|_{\mathrm{H8}} = \frac{d\gamma^p}{(2^7+1)^{1/8}} \tag{10b}$$

The anisotropy parameters and the measured shear stress and strain values were used in Eqs. (7) and (8) to generate incrementally the equivalent stress-equivalent plastic strain response of the material. It is referred to as the material frame response and is plotted in Fig. 4. Included is the corresponding response when the rotation of the material frame is not accounted for—referred to as reference frame response Clearly, this particular anisotropy leads to progressive reduction in tangent modulus for equivalent strains larger than about 0.15. Such changes in modulus can have significant influence on the prediction of localization and other instabilities and the onset of failure.

Figure 5 shows the equivalent stress–equivalent plastic strain responses corresponding to the isotropic von Mises and Hosford yield functions. Included is the reference frame response based on the Hill-48 anisotropic yield function. The three responses exhibit similar hardening, but trace different stress levels. The difference in stress level between vM and H-48 is caused by the anisotropy, whereas the difference between vM and H8 is due to the different exponent of the two yield functions.

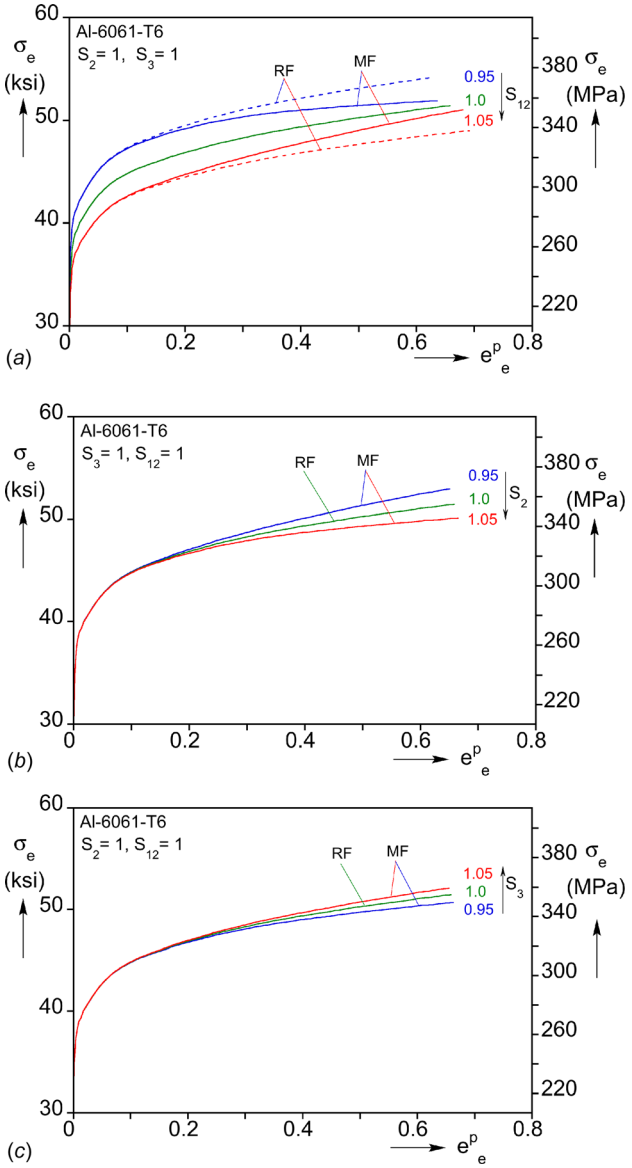

Fig. 6 Effect of anisotropy constants on the material and reference frame equivalent stress–equivalent plastic strain responses: (*a*) vary S_{12}, (*b*) vary S_2, and (*c*) vary S_3

4 Sensitivity to Anisotropy Parameters

We now conduct a limited parametric study to illustrate the effect of the anisotropy parameters, S_{ij}, on the extracted material response. The plastic tangent modulus of the material frame response is given by

$$\frac{d\sigma_e}{d\varepsilon_e^p}\Big|_{\mathrm{MF}} = \frac{d\tau}{d\gamma}\left[\frac{3}{S_{12}^2} + \left(2+\frac{2}{S_2^2}-\frac{1}{S_3^2}-\frac{3}{S_{12}^2}\right)\sin^2\gamma\right] + \frac{\tau}{2}\left(2+\frac{2}{S_2^2}-\frac{1}{S_3^2}-\frac{3}{S_{12}^2}\right)\sin 2\gamma \tag{11a}$$

By contrast in the reference frame tangent modulus is

$$\frac{d\sigma_e}{d\varepsilon_e^p}\Big|_{\mathrm{RF}} = \frac{d\tau}{d\gamma}\frac{3}{S_{12}^2} \tag{11b}$$

The measured $\tau-\gamma$ response is used together with Eqs. (3)–(8) to evaluate the material and reference frame responses for various combinations of the three anisotropy parameters. Figure 6 shows

results where each of the anisotropy parameters is varied with the other two kept at 1.0. In Fig. 6(*a*), S_{12} is assigned values of 0.95, 1.0, and 1.05. For $S_{12} = 1.0$, the material is isotropic and the response coincides with that of vM in Eq. (9). For $S_{12} = 0.95$, both the RF and MF responses are higher than the isotropic one, but this value causes the tangent modulus of the MF response to be increasingly lower than that of the RF response. When $S_{12} = 1.05$, both responses are lower than the isotropic one, but here the tangent modulus of the MF response becomes increasingly higher than that of the MF response.

In Fig. 6(*b*), S_2 is assigned values of 0.95, 1.0, and 1.05. Making this parameter larger than 1.0 lowers the tangent modulus of the MF response and making it smaller increases it. In this case, the RF response is the isotropic one. In Fig. 6(*c*), S_3 is varied in a similar manner. This parameter has the opposite effect on the RF response: $S_3 > 1.0$ increases the MF tangent modulus, while for $S_3 < 1.0$ decreases it. Here, again the RF response is the isotropic one. It is worth noting that when the anisotropy term in the round brackets in Eq. (11*a*) is larger than zero the MF response tangent modulus is larger than that of the RF tangent modulus and when it is less than zero the opposite is true.

Figure 7 shows additional comparisons of MF and RF responses for three more representative combinations of S_{ij} parameters for the same simple shear test. It is clearly demonstrated that the material frame rotation alters the response and must be accounted for. The decisive role of the anisotropy term in round brackets in Eq. (11*a*) on the hardening modulus is demonstrated here too.

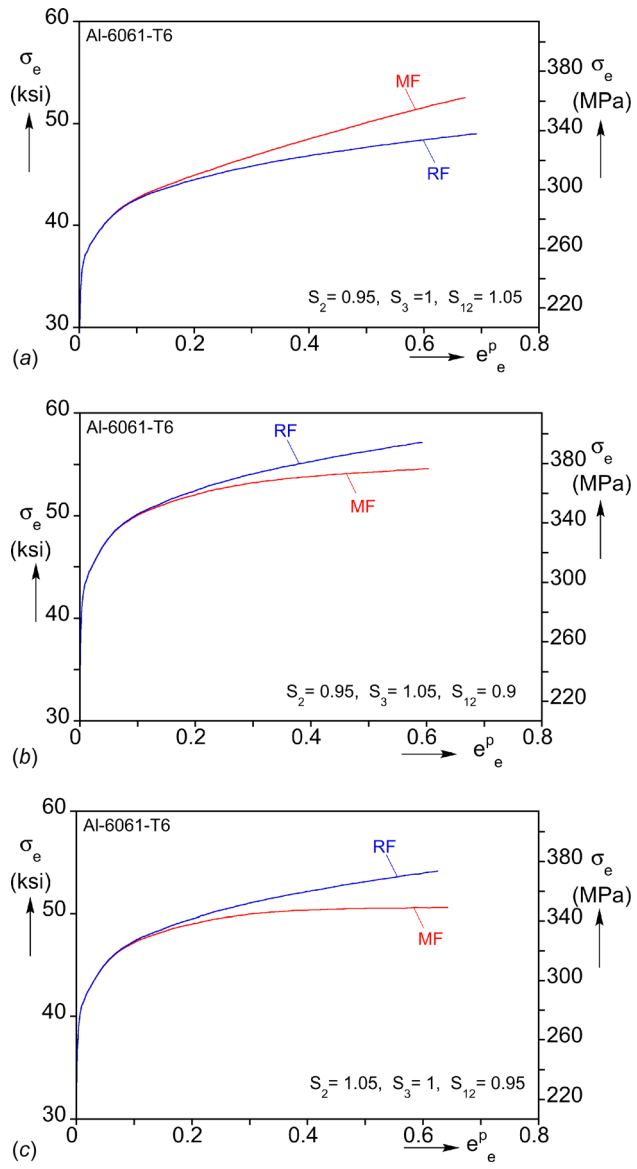

Fig. 7 Effect of anisotropy constants on the material and reference frame equivalent stress–equivalent plastic strain responses; three different combinations of S_{ij}

5 Conclusions

Numerical simulations of many manufacturing and other processes require the material response to large strains. Simple shear tests remain free of instabilities at large strains and, as a result, offer a more direct way of measuring the material response than the more traditional tensile and bulge tests. Unlike the latter two tests where the principal axes remain fixed, under simple shear the material axes rotate during deformation. This paper examined the consequences of the axes rotation on the extracted stress–strain response when the material yielding is anisotropic. The shear stress–strain response of a thin-walled Al-6061-T6 tube was measured under pure torsion. Separate sets of biaxial experiments on the same tube stock was used to calibrate the Hill-48 anisotropic yield function, which was subsequently employed to extract the material response accounting for the material axes rotation. It is demonstrated that as a consequence of the measured anisotropy, the axes rotation progressively reduces the material tangent modulus as the strain increases. The simplicity of this yield function enabled evaluation of the sensitivity of the induced changes of the extracted response to the anisotropy parameters. It is established that the material frame rotation that takes place in simple shear tests can influence the extracted response significantly when material anisotropy is accounted for, and consequently must be included in the analysis of such experiments. This conclusion also holds for alternate methods of characterizing the material anisotropy such as non-quadratic yield functions (e.g., see Ref. [7]). It is worth pointing out that the results of the analysis presented are consistent with ABAQUS' incremental treatment of the material frame rotation [14].

Acknowledgment

We also thank Dr. Raja K. Mishra of General Motors for his cooperation and technical interactions.

Funding Data

- The National Science Foundation through the GOALI (Grant No. CMMI-1663269).

References

[1] Tardif, N., and Kyriakides, S., 2012, "Determination of Anisotropy and Material Hardening for Aluminum Sheet Metal," Int. J. Solids Struct., **49**(25), pp. 3496–3506.

[2] Chen, K., Scales, M., and Kyriakides, S., 2018, "Material Hardening of a High Ductility Aluminum Alloy From a Bulge Test," Int. J. Mech. Sci., **138–139**, pp. 476–488.

[3] ASTM, 2014, "Standard Test Method for Shear Testing of Thin Aluminum Alloy Products," ASTM International, West Conshohocken, PA, Standard No. ASTM B831.

[4] Miyauchi, K., 1984, "A Proposal of a Planar Simple Shear Test in Sheet Metals," Sci. Papers Inst. Phys. Chem. Res. (Jpn.), **87**, pp. 27–40.

[5] Marciniak, Z., 1961, "Influence of the Sign Change of the Load on the Strain Hardening Curve of a Copper Test Subject to Torsion," Arch. Mech. Stosowanj, **13**, pp. 743–751.

[6] Yin, Q., Zillmann, B., Suttner, S., Gerstein, G., Biasutti, M., Tekkaya, A. E., Wagner, M. F. X., Merklein, M., Schaper, M., Halle, T., and Brosius, A., 2014, "An Experimental and Numerical Investigation of Different Shear Test Configurations for Sheet Metal Characterization," Int. J. Solids Struct., **51**(5), pp. 1066–1074.

[7] Barlat, F., Aretz, H., Yoon, J. W., Karabin, M. E., Brem, J. C., and Dick, R. E., 2005, "Linear Transformation-Based Anisotropic Yield Functions," Int. J. Plast., **21**(5), pp. 1009–1039.

[8] Kang, J., Wilkinson, D. S., Wu, P. D., Bruhis, M., Jain, M., Embury, J. D., and Mishra, R. K., 2008, "Constitutive Behavior of AA5754 Sheet Materials at Large Strains," ASME J. Eng. Mater. Technol., **130**(3), p. 031004.
[9] Abedini, A., Butcher, C., Rahmaan, T., and Worswick, M. J., 2017, "Evaluation and Calibration of Anisotropic Yield Criteria in Shear Loading: Constraints to Eliminate Numerical Artefacts," Int. J. Solids Struct., (in press).
[10] Hill, R., 1950, *The Mathematical Theory of Plasticity*, Clarendon Press, Oxford, UK.
[11] Scales, M., Tardif, N., and Kyriakides, S., 2016, "Ductile Failure of Aluminum Alloy Tubes Under Combined Torsion and Tension," Int. J. Solids Struct., **97–98**, pp. 116–128.
[12] Hill, R., 1948, "A Theory of the Yielding and Plastic Flow of Anisotropic Metals," Proc. R. Soc. Lond. A, **193**(1033), pp. 281–297.
[13] Hosford, W. F., 1972, "A Generalized Isotropic Yield Criterion," ASME J. Appl. Mech., **39**(2), pp. 607–609.
[14] ABAQUS, 2016, "ABAQUS Theory Guide Section 1.4.3," Dassault Systèmes Simulia Corp., Providence, RI.